

Multi-Modal Hypergraph Diffusion Network with Dual Prior for Alzheimer Classification

Angelica I. Aviles-Rivero¹, Christina Runkel¹, Nicolas Papadakis²,
Zoe Kourtzi³, and Carola-Bibiane Schönlieb^{1*}

¹ DAMTP, University of Cambridge, UK {ai323,cr661,cbs31}@cam.ac.uk

² IMB, Université de Bordeaux, France nicolas.papadakis@math.u-bordeaux.fr

³ Department of Psychology, University of Cambridge, UK zk240@cam.ac.uk

Abstract. The automatic early diagnosis of prodromal stages of Alzheimer’s disease is of great relevance for patient treatment to improve quality of life. We address this problem as a multi-modal classification task. Multi-modal data provides richer and complementary information. However, existing techniques only consider either lower order relations between the data and single/multi-modal imaging data. In this work, we introduce a novel semi-supervised hypergraph learning framework for Alzheimer’s disease diagnosis. Our framework allows for higher-order relations among multi-modal imaging and non-imaging data whilst requiring a tiny labelled set. Firstly, we introduce a dual embedding strategy for constructing a robust hypergraph that preserves the data semantics. We achieve this by enforcing perturbation invariance at the image and graph levels using a contrastive based mechanism. Secondly, we present a dynamically adjusted hypergraph diffusion model, via a semi-explicit flow, to improve the predictive uncertainty. We demonstrate, through our experiments, that our framework is able to outperform current techniques for Alzheimer’s disease diagnosis.

Keywords: Hypergraph Learning · Multi-Modal Classification · Semi-Supervised Learning · Augmentation Invariance · Alzheimer’s disease.

1 Introduction

Alzheimer’s disease (AD) is an irreversible, neurodegenerative disease impairing memory, language and cognition [9]. It starts slowly but progressively worsens and causes approximately 60-80% of all cases of dementia [4]. As there is no cure available yet, detecting the disease as early as possible, in prodromal stages, is crucial for slowing down its progression and for patient to improve quality of life. The body of literature has show the potentials of existing machine learning methods e.g., [28,20,30,26]. However, there are two major limitations of existing techniques. Firstly, incorporating other relevant data types such as phenotypic data in combination with large-scale imaging data has shown to be beneficial e.g. [19]. However, existing approaches fail to exploit the rich available imaging

* the Alzheimer’s Disease Neuroimaging Initiative

and non-imaging data. This is mainly due to the inherent problem of how to provide better and higher relations between multi-modal sources. Secondly, whilst vast amount of data is acquired every day at hospitals, labelling is expensive, time-consuming and prone to human bias. Therefore, to develop models that rely on extreme minimal supervision is of a great interest in the medical domain.

To address the aforementioned problems, hypergraph learning has been explored – as it allows going beyond pair-wise data relations. In particular, hypergraphs have already been explored for the task of AD diagnosis e.g. [18,32,24,25]. From the machine learning perspective [6], several works have addressed the problem of hypergraph learning, by generalising the graph Laplacian to hypergraphs e.g. [31,22,15,23]. The principles from such techniques opened the door to extend the hypergraph Laplacian to graph neural networks (GNNs) e.g. [27,11]. However, the commonality of existing hypergraph techniques for AD diagnosis, and in general in the ML community, is that they consider the clique/star expansion [2], and in particular, follow the hypergraph normalised cut of that [31].

To tackle the aforementioned challenges, we introduce a novel semi-supervised hypergraph learning framework for Alzheimer’s disease diagnosis. Our work follows a hybrid perspective, where we propose a new technique based on a dual embedding strategy and a diffusion model. To the best of our knowledge, this is the first work that explores invariance at the image and graph levels, and goes beyond the go-to technique of [31] by introducing a better hypergraph functional.

Our contributions are as follows. 1) We introduce a self-supervised dual multi-modal embedding strategy. The framework enforces invariance on two spaces– the manifold that lies the imaging data and the space of the hypergraph structure. Our dual strategy provides better priors on the data distribution, and therefore, we construct a robust graph that offers high generalisation capabilities. 2) In contrast to existing techniques that follow [31], we introduce a more robust diffusion-model. Our model is based on the Rayleigh quotient for hypergraph p -Laplacian and follows a semi-explicit flow.

2 Proposed Framework

In this section, we introduce our semi-supervised hypergraph learning framework (see Figure 1). We highlight two key parts of our approach: i) our dual embedding strategy to construct a robust graph, and ii) our dynamically adaptive hypergraph diffusion model.

2.1 Hypergraph Embeddings & Construction

The first part of our framework addresses a major challenge in hypergraph learning – that is, how to extract meaningful embeddings, from the different given modalities, to construct a robust hypergraph. The most recent works for Alzheimer’s disease diagnosis are based on extracting embeddings using sparse constraints or directly from a deep network. However, existing works only consider data level features to construct a graph or hypergraph and mainly for

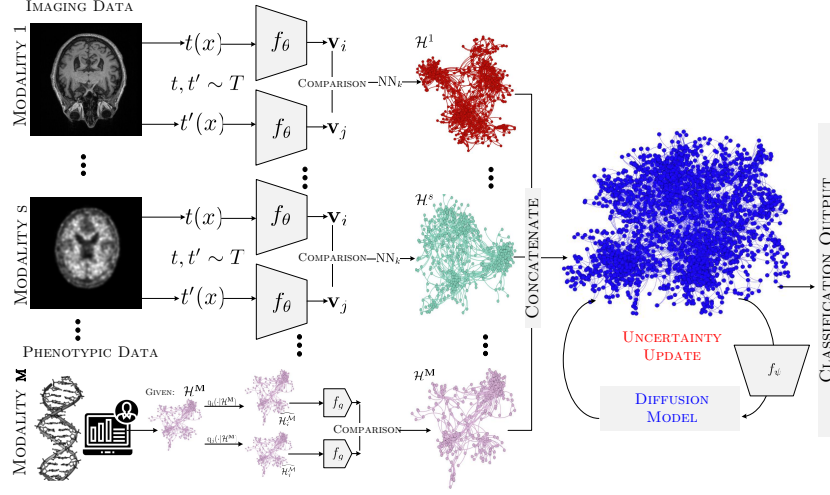


Fig. 1: Visual illustration of our framework. We first use a dual embeddings strategy at the image and hypergraph level. We then introduce a diffusion model for predicting early diagnosis of prodromal stages of Alzheimer’s disease.

imaging data. In contrast to existing works, we allow for higher-order relations between multi-modal imaging and non-imaging data. Secondly, we enforce a dual perturbation invariance strategy at both image and graph levels. With our dual multi-modal embedding strategy, *we seek to provide better priors on the data distribution such as our model is invariant to perturbations, and therefore, we can construct a robust graph that offers high generalisation capabilities.*

We consider a hypergraph as a tuple $\mathcal{G} = (\mathcal{V}, \mathcal{E}, w)$, where $\mathcal{V} = \{v_1, \dots, v_n\}$, $|\mathcal{V}| = n$ is a set of nodes and $\mathcal{E} = \{e_1, \dots, e_m\}$, $|\mathcal{E}| = m$ the hyperedges. Moreover, $w : \mathcal{E} \rightarrow \mathbb{R}_{>0}$ refers to the hyperedges weights, in which each hyperedge e is associated to a subset of nodes. The associated incidence matrix is given by $\mathcal{H}_{i,e} = \begin{cases} 1 & \text{if } i \in e, \\ 0 & \text{otherwise} \end{cases}$, where $i \in \mathcal{V}$ and e is an hyperedge; *i.e.* a subset of nodes of \mathcal{V} . In our multi-modal setting, we assume a given \mathbf{M} modalities. We have for each modality N samples $X = \{x_1, \dots, x_N\} \in \mathcal{X}$ sampled from a probability distribution \mathbb{P} on \mathcal{X} . We then have a multi-modal data collection as $\{X_1, \dots, X_s, X_{s+1}, \dots, X_M\}$. The first s modalities are imaging data (e.g. PET imaging) whilst the remaining are non-imaging data (e.g. genetics).

The first problem we address in our framework is how to learn embeddings, $\mathbf{v} = f_\theta(x)$, without supervision and invariant to perturbations. That is, given a deep network f_θ , with parameters θ , we seek to map the imaging/non-imaging sample x to a feature space \mathbf{v} . As we seek to obtain relevant priors on the data distribution, we also consider a group of T transformations such as there exists a representation function $\phi : T \times \mathcal{X} \rightarrow \mathcal{X}$, $(t, x) \mapsto \phi(t, x)$. We then seek to enforce

$\phi(t, x) = \phi(x)$ for all $t \in T$. We divide our embedding learning problem into two strategies corresponding to each type of data.

For the imaging data, we use contrastive self-supervised learning (e.g. [13,14,7]) for mapping X to a feature space $\mathbf{v} = \{\mathbf{v}_1, \dots, \mathbf{v}_N\}$ with $\mathbf{v}_i = f_\theta(x_i)$ such that \mathbf{v}_i better represents x_i . Given $t(x_i)$ and $t'(x_i)$, where $t, t' \sim T$ are operators that produce two perturbed versions of the given sample (defined following [8]), we seek to learn a batch of embeddings that are invariant to any transformation (see Figure 2). Formally, we compute the following contrastive loss:

$$\mathcal{L}_{visual}^{(i,j), X_{i \in s}} = -\log \frac{\exp(\mathbf{f}_{i,j}/\tau)}{\sum_{k=1}^n \mathbb{1}_{[k \neq i]} \exp(\mathbf{f}_{i,k}/\tau)}, \text{ where } \mathbf{f}_{i,j} = \frac{\mathbf{v}_i^T \mathbf{v}_j}{\|\mathbf{v}_i\| \cdot \|\mathbf{v}_j\|}, \quad (1)$$

where $\tau > 0$ is a temperature hyperparameter and $\mathbf{f}_{i,k}$ follows same cosine similarity definition than $\mathbf{f}_{i,j}$. We denote the k -nearest neighbors of an embedding \mathbf{v}_i as $\text{NN}_k(\mathbf{v}_i)$. We then construct for each X_1, \dots, X_s a corresponding hypergraph $\mathcal{H}_{ij}^{1, \dots, s} = [\mathbf{v}_i^T \mathbf{v}_j]$ if $\mathbf{v}_i \in \text{NN}_k(\mathbf{v}_j)$, otherwise 0.

For the non-imaging data (e.g. genetics and age), we follow different protocol as perturbing directly the data might neglect the data/structure semantics. We then seek to create a subject-phenotypic relation. To do this, we compute the similarity between the subjects \mathbf{x} and the corresponding phenotypic measures, to generate the hypergraphs $\mathcal{H}^{s+1, \dots, M}$. Given a set of phenotypic measures, we compute a NN_k graph between subjects given the set of measures \mathbf{z} such as $S(\mathbf{x}, \mathbf{z})$ if $\mathbf{x} \in \text{NN}_k(\mathbf{z})$, otherwise 0; being S a similarity function. That is, we enforce the connection of subjects within similar phenotypic measures. We then

seek to perturb $\mathcal{H}^{s+1, \dots, M}$ such that the transformed versions $\hat{\mathcal{H}}^{s+1, \dots, M} \sim \mathbf{q}(\hat{\mathcal{H}}^{s+1, \dots, M} | \mathcal{H}^{s+1, \dots, M})$ where $\mathbf{q}(\cdot)$ refers to the transformation drawn from the distribution of the given measure. Our set of transformations are node dropping and edge perturbation. We follow, for the group of transformations T , the ratio and dropping probability strategies of [21,29]. To maximise the agreement between the computed transformation, we use the same contrastive loss as defined in (1). We denote the loss as $\mathcal{L}_{pheno}^{(i,j), \mathcal{H}^{s+1, M}}$ for non-imaging data. The final hypergraph, \mathcal{H} , is the result of concatenating all hypergraph structures from all modalities, $\mathcal{H}^1, \dots, \mathcal{H}^M$ given by both imaging and non-imaging data.

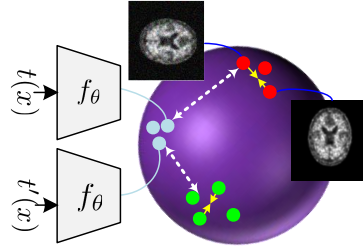


Fig. 2: We seek for distinctiveness. Related samples should have similar features.

2.2 Dynamically Adjusted Hypergraph Diffusion Model

The second key part of our framework is a semi-supervised hypergraph diffusion model. After constructing a robust hypergraph, we now detail how we perform disease classification using only a tiny labelled set.

We consider a small amount of labelled data $X_L = \{(x_i, y_i)\}_{i=1}^l$ with provided labels $\mathcal{L} = \{1, \dots, L\}$ and $y_i \in \mathcal{L}$ along with a large unlabelled set $X_u = \{x_k\}_{k=l+1}^m$. The entire dataset is then $X = X_L \cup X_u$. The goal is to use the provided labeled data X_L to infer a function, $f : \mathcal{X} \mapsto \mathcal{Y}$, that maps the unlabelled set to class labels. However, to obtain such mapping efficiently and with minimum generalisation error is even more challenging when using multi-modal data e.g. [19]. We cast this problem as a label diffusion process on hypergraphs.

We consider the problem of hypergraph regularisation for semi-supervised classification [31,15,11], where we aim to find a function u^* to infer labels for the unlabelled set and enforce smoothness on the hypergraph. We seek to solve a problem of the form $u^* = \operatorname{argmin}_{u \in \mathbb{R}^{|V|}} \{\mathcal{L}_{emp}(u) + \gamma \Omega(u)\}$, where u $\mathcal{L}_{emp}(u)$ refers to an empirical loss (e.g., square loss), $\Omega(u)$ denotes a regulariser and $\gamma > 0$ is a weighting parameter balancing the importance of each term. Whilst majority of works consider the clique/star expansion [2] and follow the principles of [22,31], *we seek to provide a more robust functional* to avoid the inherent disadvantages of such approximations (e.g. bias during the graph diffusion [15]). In particular, we consider the setting of Rayleigh quotient for p -Laplacian. We then seek to estimate, for $p = 1$, the particular family of solutions based on the minimisation of the ratio $\Omega(u) = \frac{TV_H(u)}{\|u\|}$, where $TV_H = \sum_{e \in \mathcal{E}} w_e \max_{i,j \in e} |u_i - u_j|$ is the total variation functional on the hypergraph. To do this, we generalise [10] to a hypergraph setting and introduce a dynamic adjustment on the diffusion model, which is based on controlling the predictive uncertainty. Our framework allows for both binary and multi-class classification settings. Given a number of epochs $E \in [1, \dots, E]$ and following previous notation, we compute an alternating optimisation process as follows.

Alternating Optimisation for Epoch $\in [1, \dots, E]$:

SUB-PROBLEM 1: DIFFUSION MODEL MINIMISATION. For a given label, we define a function $u \in \mathbb{R}^n$ over the nodes, and denote its value at node x as $u(x)$. In this binary setting, the objective is to estimate a function u that denotes the presence (resp. absence) of the label for data x . To that end, following [10], we seek to solve $\min \frac{TV_H(u)}{\|u\|}$ with the following semi-explicit flow, in which u_k is the u value at iteration k :

$$\text{Diffusion Model} \begin{cases} \frac{u_{k+1/2} - u_k}{\delta t} = \frac{TV_H(u_k)}{\|u_k\|} (q_k - \tilde{q}_k) - \phi_{k+1/2}, \\ u_{k+1} = \frac{u_{k+1/2}}{\|u_{k+1/2}\|_2} \end{cases} \quad (2)$$

where $\phi_{k+1/2} \in \partial TV_H(u_{k+1/2})$, $q \in \partial \|u_k\|$ (with ∂f the set of possible subdifferentials of a convex function f defined as $\partial f = \{\phi, \text{ s.t. } \exists u, \text{ with } \phi \in \partial f(u)\}$), the scaling $d(x)$ is such that $\tilde{q}_k = \frac{\langle d, q_k \rangle}{\langle d, d \rangle} d$, and δt is a positive time step. Once the PDE has converged, the output of (2) is a bivalued function that can be threshold to perform a binary partition of the hypergraph. In order to realise a multi-class labelling, we consider the generalised model of [5] that includes as prior the available labels of X_L in $\mathcal{L}_{emp}(u)$ to guide the partitioning and estimates L coupled functions $u^l(x)$ $l = 1, \dots, L$. The final labeling is computed as $\hat{y}_i = \operatorname{argmax}_{i \in \{1, \dots, L\}} u^l(x)$ with $L(x) \in \hat{y}_i$. *Intuition:* Having our constructed

hypergraph as in subsection 2.1, we seek to use a tiny labelled set, as we are in a semi-supervised setting, to diffuse the labels for the unlabelled set. A major challenge in semi-supervised learning is how to reduce the prediction bias (e.g. [3]) for the unlabelled set, as it is conditioned solely to the tiny labelled set as prior. We then seek to update the uncertainty of the computed \hat{y}_i via solving Sub-Problem 2.

SUB-PROBLEM 2: UNCERTAINTY HYPERGRAPH MINIMISATION. Following the scheme from Figure 1 and notation from previous sections, we first initialise f_ψ using the tiny labelled set available, X_L , and then we take \hat{y}_i from Sub-Problem 1 and check the uncertainty of \hat{y}_i by computing the following loss:

$$\mathcal{L}_{DYN}(X, Y, \hat{Y}; \theta) := \min_{\theta} \sum_{i=1}^l \mathcal{L}_{CE}(f_{\theta}(x_i), y_i) + \sum_{i=l+1}^m \gamma_i \mathcal{L}_{CE}(f_{\theta}(x_i), \hat{y}_i), \quad (3)$$

where \mathcal{L}_{CE} is a cross entropy loss and γ is the measure of uncertainty via entropy [17,1] defined as $\gamma_i = 1 - (H(u_{\hat{y}_i})/\log(L))$, where H refers to the entropy and $u_{\hat{y}_i}$ is normalised beforehand. *Intuition:* From previous step, we obtain an initial prediction for the unlabelled set on the hypergraph. However, in semi-supervised learning due to the tiny labelled set as prior, the unlabelled data tend to have an asymptotic bias in the prediction. We then ensure that there is a high certainty in the unlabelled predictions since early epochs to avoid the propagation of incorrect predictions.

3 Experimental Results

In this section, we provide all details of our evaluation protocol.

Data Description. We evaluate our semi-supervised hypergraph framework using the Alzheimer’s disease Neuroimaging Initiative (ADNI) dataset¹. ADNI is a multi-centre dataset composed of multi-modal data including imaging and multiple phenotype data. We consider 500 patients using MRI, PET, demographics and Apolipoprotein E (APOE). We included APOE as it is known to be a crucial genetic risk factor for developing Alzheimer’s disease. The dataset contains four categories: early mild cognitive impairment (EMCI), late mild cognitive impairment (LMCI), normal control (NC) and Alzheimer’s disease (AD).

Evaluation Protocol. We design a three part evaluation scheme. Firstly, we follow the majority of techniques convention for binary classification comparing AD vs NC, AD vs EMCI, AD vs LMCI, EMCI vs NC, LMCI vs NC and EMCI vs LMCI (see Supplementary Material for extended results). Secondly, we extended the classification problem to a multi-class setting including the four classes AD vs NC vs EMCI vs LMCI. We consider this setting, as one of the major challenges in AD diagnosis is to fully automate the task without pre-selecting classes [12].

¹ Data used were obtained from the Alzheimer’s Disease Neuroimaging Initiative (ADNI) database (adni.loni.usc.edu)

TECHNIQUE	AD vs NC			EMCI vs LMCI		
	ACC	SEN	PPV	SEN	PPV	ACC
GNNs [19]	81.60±2.81	83.20±3.10	80.62±2.30	75.60±2.50	75.20±3.02	75.80±2.45
HF [24]	87.20±2.10	88.01±2.15	86.60±2.60	80.40±2.02	82.41±2.14	79.23±2.60
HGSCCA [25]	85.60±2.16	87.20±3.11	84.40±2.15	76.01±2.16	75.21±2.01	76.42±2.22
HGNN [11]	88.01±2.60	90.40±2.16	87.59±2.42	80.60±2.05	81.60±2.54	79.60±2.51
DHGNN [16]	89.90±2.40	89.60±2.15	90.21±2.45	80.80±2.47	82.40±2.41	79.80±2.76
Ours	92.11±2.03	92.80±2.16	91.33±2.43	85.22±2.25	86.40±2.11	84.02±2.45

Table 1: Numerical comparison of our technique and existing (graph) and hypergraph techniques. All comparison are run on same conditions. The best results are highlighted in green colour.

TECHNIQUE	LMCI vs NC		
	ACC	SEN	PPV
GNNs [19]	72.40±2.05	70.40±2.80	73.30±2.04
HF [24]	77.01±2.26	77.6±2.15	78.22±2.51
HGSCCA [25]	74.00±2.10	74.40±2.16	73.80±2.17
HGNN [11]	78.90±3.01	80.01±2.7	78.10±2.67
DHGNN [16]	79.20±2.70	80.03±3.01	78.74±3.22
Ours	82.01±2.16	84.01±2.34	81.80±2.55

Table 2: Performance comparison of our technique and existing hypergraph models for LMCI vs NC. The results in green colour denotes the highest performance.

To evaluate our model, we performed comparisons with state-of-the-art techniques on hypergraph learning: HF [24], HGSCCA [25], HGNN [11] and DHGNN [16]. We also added the comparison against GNNs [19], which is based on graph neural networks (GNNs). We added this comparison as it also considers imaging and non-imaging data. For a fair comparison in performance, we ran those techniques under same conditions. The quality check is performed following standard convention in the medical domain: accuracy (ACC), sensitivity (SEN), and positive predictive value (PPV) as a trade-off metric between sensitivity and specificity. Moreover and guided by the field of estimation statistics, we report along with the error rate the confidence intervals (95%) when reporting multi-class results. We set the k-NN neighborhood to $k = 50$, for the alternating optimisation we used a weight decay of 2×10^{-4} and learning rate was set to 5e-2 decreasing with cosine annealing, and use 180 epochs. For the group of transformations T , we use the strategy of that [8] for the imaging data whilst for the non-imaging data the ratio and dropping probability strategies of [21,29]. Following standard protocol in semi-supervised learning, we randomly select the labelled samples

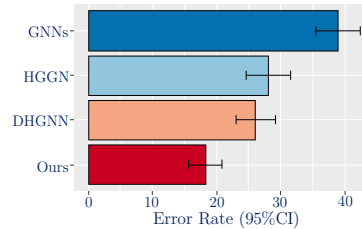


Fig. 3: Performance comparison for the four classes case.

TECHNIQUE	AD vs NC vs MCI	AD vs NC vs EMCI vs LMCI
	ERROR RATE & 95%CI	ERROR RATE & 95%CI
GNNs [19]	36.19±4.45	39.01±3.12
HGNN [11]	26.35±3.20	28.09±3.65
DHGNN [16]	23.10±2.60	26.25±2.55
Ours	16.25±2.22	18.31±2.45

Table 3: Error rate comparison of our technique against existing models. The results in green denotes the best performance.

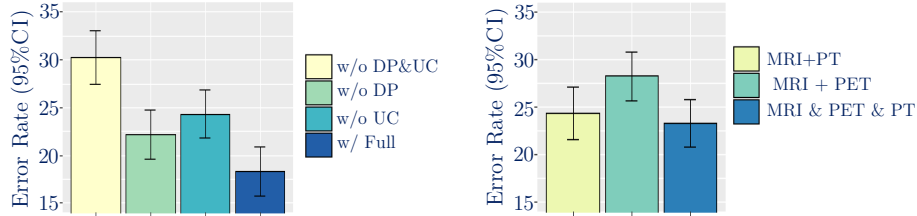


Fig. 4: (left side) Ablation study for the components of our technique. (right side) Performance comparison using different type of multi-modal data.

over five repeated time and then report the mean of the metrics along with the standard deviation.

Results & Discussion. We began by evaluating our framework following the binary comparison of AD vs NC, EMCI vs LMCI and LMCI vs NC (see supplementary material for extended results). We report a detailed quantitative analysis to understand the performance of ours and compared techniques. We use 15% of labelled data (see supplementary material). The results are reported in Tables 1 & 2. In a closer look at the results, we observe that our technique reports the best performance for all comparison and in all metrics. We also observe that the GNNs [19] reported the worst performance. This is due to the fact that GNNs does not allow for higher-order relations on the graph. We highlight that whilst the other techniques reported a good performance, our technique substantially improved over all methods (with statistical significance, see supplementary material). We underline that all compared techniques follows the hypergraph approximation of [31], which is bias during the hypergraph partition. We showed that our diffusion model, that follows different principles, mitigates that problem.

To further support our previous results, we also report results in the more challenging setting of multi-class classification for AD diagnosis. The results are reported in Table 3. We observe that our technique performance is consistent with previous results. That is, our technique reported the lowest error rate for both multi-class cases. Our technique decreased the error rate for more than 40% for all techniques. Figure 3 complements these results by reporting the performance with respect to the four classes case.

Finally, to support the design of our technique, we performed two ablations studies regarding our design and the modalities used. We start by evaluating

the influence of our full model against without our dual perturbed embedding strategy (displayed as DP) and our uncertainty (denoted as UC) scheme. The results are reported at the left side of Figure 4 on the four classes case. Whilst our dual strategy substantially improves the performance, we observe that our uncertainty scheme has a major repercussion. The intuition is that our diffusion model ensures, at early epochs, that there is a high certainty in the prediction avoiding incorrect prediction in subsequent epochs. We also include an ablation study regarding the impact of the modalities (PT refers to phenotypic data). From the right side of Figure 4, we observe that including phenotypic data has a greater positive impact on the performance than using only imaging data.

4 Conclusion

We proposed a novel semi-supervised hypergraph framework for Alzheimer’s disease diagnosis. Unlike existing techniques, we introduce a dual embedding strategy. As phenotypic data highly differs from imaging data. Moreover, in contrast to existing techniques that follow the hypergraph approximation of [31]. We introduce a better diffusion model, which solution is provided by a semi-explicit flow in the fra hypergraph learning. From our results, we showed that our technique outperforms other hypergraph techniques. Future work includes a more extensive clinical evaluation with public and in-home datasets.

Acknowledgements AIAR gratefully acknowledges support from CMIH and CCIMI, University of Cambridge. CR acknowledges support from the CCIMI and the EPSRC grant Nr. EP/W524141/1 reference 2602161. ZK acknowledges support from the BBSRC (H012508 and BB/P021255/1), Alan Turing Institute (TU/B/000095), Wellcome Trust (205067/Z/16/Z, 221633/Z/20/Z) and Royal Society (INF/R2/202107). CBS acknowledges support from the Philip Leverhulme Prize, the Royal Society Wolfson Fellowship, the EPSRC advanced career fellowship EP/V029428/1, EPSRC grants EP/T003553/1, EP/N014588/1, the Wellcome Trust 215733/Z/19/Z and 221633/Z/20/Z, Horizon 2020 under the Marie Skłodowska-Curie No. 777826 NoMADS, the CCIMI and the Alan Turing Institute.

References

1. Abdar, M., Pourpanah, F., Hussain, S., Rezazadegan, D., Liu, L., Ghavamzadeh, M., Fieguth, P., Cao, X., Khosravi, A., Acharya, U.R., et al.: A review of uncertainty quantification in deep learning: Techniques, applications and challenges. *Information Fusion* **76**, 243–297 (2021)
2. Agarwal, S., Branson, K., Belongie, S.: Higher order learning with graphs. In: *Proceedings of the 23rd international conference on Machine learning*. pp. 17–24 (2006)
3. Arazo, E., Ortego, D., Albert, P., O’Connor, N.E., McGuinness, K.: Pseudo-labeling and confirmation bias in deep semi-supervised learning. In: *2020 International Joint Conference on Neural Networks (IJCNN)*. pp. 1–8. IEEE (2020)

4. Association, A.: What is alzheimer's disease? (2022)
5. Aviles-Rivero, A.I., Papadakis, N., Li, R., Sellars, P., Fan, Q., Tan, R.T., Schönlieb, C.B.: Graphxnet - chest x-ray classification under extreme minimal supervision. In: International Conference on Medical Image Computing and Computer-Assisted Intervention. pp. 504–512. Springer (2019)
6. Berge, C.: Hypergraphs: combinatorics of finite sets, vol. 45. Elsevier (1984)
7. Chen, T., Kornblith, S., Norouzi, M., Hinton, G.: A simple framework for contrastive learning of visual representations. In: International conference on machine learning. pp. 1597–1607. PMLR (2020)
8. Cubuk, E.D., Zoph, B., Shlens, J., Le, Q.V.: Randaugment: Practical automated data augmentation with a reduced search space. In: Proceedings of the IEEE/CVF Conference on Computer Vision and Pattern Recognition Workshops. pp. 702–703 (2020)
9. De Strooper, B., Karran, E.: The cellular phase of alzheimer's disease. *Cell* **164**(4), 603–615 (2016)
10. Feld, T., Aujol, J.F., Gilboa, G., Papadakis, N.: Rayleigh quotient minimization for absolutely one-homogeneous functionals. *Inverse Problems* **35**(6), 064003 (2019)
11. Feng, Y., You, H., Zhang, Z., Ji, R., Gao, Y.: Hypergraph neural networks. In: Proceedings of the AAAI Conference on Artificial Intelligence. vol. 33, pp. 3558–3565 (2019)
12. Goenka, N., Tiwari, S.: Deep learning for alzheimer prediction using brain biomarkers. *Artificial Intelligence Review* **54**(7), 4827–4871 (2021)
13. Hadsell, R., Chopra, S., LeCun, Y.: Dimensionality reduction by learning an invariant mapping. In: 2006 IEEE Computer Society Conference on Computer Vision and Pattern Recognition (CVPR'06). vol. 2, pp. 1735–1742. IEEE (2006)
14. He, K., Fan, H., Wu, Y., Xie, S., Girshick, R.: Momentum contrast for unsupervised visual representation learning. In: Proceedings of the IEEE/CVF conference on computer vision and pattern recognition. pp. 9729–9738 (2020)
15. Hein, M., Setzer, S., Jost, L., Rangapuram, S.S.: The total variation on hypergraphs-learning on hypergraphs revisited. *Advances in Neural Information Processing Systems* **26** (2013)
16. Jiang, J., Wei, Y., Feng, Y., Cao, J., Gao, Y.: Dynamic hypergraph neural networks. In: IJCAI. pp. 2635–2641 (2019)
17. Kendall, A., Gal, Y.: What uncertainties do we need in bayesian deep learning for computer vision? *Advances in neural information processing systems* (2017)
18. Pan, J., Lei, B., Shen, Y., Liu, Y., Feng, Z., Wang, S.: Characterization multimodal connectivity of brain network by hypergraph gan for alzheimer's disease analysis. In: Chinese Conference on Pattern Recognition and Computer Vision (PRCV). pp. 467–478. Springer (2021)
19. Parisot, S., Ktena, S.I., Ferrante, E., Lee, M., Guerrero, R., Glocker, B., Rueckert, D.: Disease prediction using graph convolutional networks: application to autism spectrum disorder and alzheimer's disease. *Medical image analysis* **48**, 117–130 (2018)
20. Pölsterl, S., Aigner, C., Wachinger, C.: Scalable, axiomatic explanations of deep alzheimer's diagnosis from heterogeneous data. In: International Conference on Medical Image Computing and Computer-Assisted Intervention. pp. 434–444. Springer (2021)
21. Qiu, J., Chen, Q., Dong, Y., Zhang, J., Yang, H., Ding, M., Wang, K., Tang, J.: Gcc: Graph contrastive coding for graph neural network pre-training. In: Proceedings of the 26th ACM SIGKDD International Conference on Knowledge Discovery & Data Mining. pp. 1150–1160 (2020)

22. Rodriguez, J.A.: On the laplacian eigenvalues and metric parameters of hypergraphs. *Linear and Multilinear Algebra* **50**(1), 1–14 (2002)
23. Saito, S., Mandic, D., Suzuki, H.: Hypergraph p-laplacian: A differential geometry view. In: *Proceedings of the AAAI Conference on Artificial Intelligence*. vol. 32 (2018)
24. Shao, W., Peng, Y., Zu, C., Wang, M., Zhang, D., Initiative, A.D.N., et al.: Hyper-graph based multi-task feature selection for multimodal classification of alzheimer’s disease. *Computerized Medical Imaging and Graphics* **80**, 101663 (2020)
25. Shao, W., Xiang, S., Zhang, Z., Huang, K., Zhang, J.: Hyper-graph based sparse canonical correlation analysis for the diagnosis of alzheimer’s disease from multi-dimensional genomic data. *Methods* **189**, 86–94 (2021)
26. Shin, H.C., Ihsani, A., Xu, Z., Mandava, S., Sreenivas, S.T., Forster, C., Cha, J., Initiative, A.D.N., et al.: Gandalf: Generative adversarial networks with discriminator-adaptive loss fine-tuning for alzheimer’s disease diagnosis from mri. In: *International Conference on Medical Image Computing and Computer-Assisted Intervention*. pp. 688–697. Springer (2020)
27. Yadati, N., Nimishakavi, M., Yadav, P., Nitin, V., Louis, A., Talukdar, P.: Hypergc: A new method for training graph convolutional networks on hypergraphs. *Advances in neural information processing systems* **32** (2019)
28. Yang, F., Meng, R., Cho, H., Wu, G., Kim, W.H.: Disentangled sequential graph autoencoder for preclinical alzheimer’s disease characterizations from adni study. In: *International Conference on Medical Image Computing and Computer-Assisted Intervention*. pp. 362–372. Springer (2021)
29. You, Y., Chen, T., Sui, Y., Chen, T., Wang, Z., Shen, Y.: Graph contrastive learning with augmentations. *Advances in Neural Information Processing Systems* **33**, 5812–5823 (2020)
30. Zhou, B., Wang, R., Chen, M.K., Mecca, A.P., O’Dell, R.S., Dyck, C.H.V., Carson, R.E., Duncan, J.S., Liu, C.: Synthesizing multi-tracer pet images for alzheimer’s disease patients using a 3d unified anatomy-aware cyclic adversarial network. In: *International Conference on Medical Image Computing and Computer-Assisted Intervention*. pp. 34–43. Springer (2021)
31. Zhou, D., Huang, J., Schölkopf, B.: Learning with hypergraphs: Clustering, classification, and embedding. *Advances in neural information processing systems* **19** (2006)
32. Zuo, Q., Lei, B., Shen, Y., Liu, Y., Feng, Z., Wang, S.: Multimodal representations learning and adversarial hypergraph fusion for early alzheimer’s disease prediction. In: *Chinese Conference on Pattern Recognition and Computer Vision (PRCV)*. pp. 479–490. Springer (2021)